Applied Energy 183 (2016) 390–398

Contents lists available at ScienceDirect

Applied Energy

journal homepage: www.elsevier.com/locate/apenergy

Novel state-of-health diagnostic method for Li-ion battery in service

R. Mingant *, J. Bernard, V. Sauvant-Moynot

IFP Energies nouvelles, Rond-point de l'échangeur de Solaize, BP 3, 69360 Solaize, France

HIGHLIGHTS

- Two modules of 66 cells were aged with two EV cycling protocols.
- Free ageing signals (U,I) were used to determine the quasi-EIS (QEIS) spectra.
- These QEIS spectra were fitted with an equivalent circuit model.
- The fitted parameters were used to develop a tool to estimate the battery SoH.
- This tool shows good accuracy in the estimation of SoH (2% uncertainty).

ARTICLE INFO

Article history:
Received 6 June 2016
Received in revised form 18 August 2016
Accepted 19 August 2016

Keywords:
Li-ion battery
Lithium Iron Phosphate-graphite (LFP-C)
Ageing
State of Health (SOH)
Fast Fourier Transform (FFT)
Electrochemical Impedance Spectroscopy (EIS)

ABSTRACT

The development of improved State-of-Health (SoH) diagnostic methods is a current research topic for battery-powered applications. For instance, the current rapid development of Electric Vehicles (EV) creates a strong demand for an accurate and reliable on-board SoH indicator during operation. Such an indicator is a key parameter required to optimize battery energy management and to track the degradation of the system performance. The electrochemical impedance spectrum (EIS) of an electrochemical system is a powerful lab-based diagnostic technique, usually measured using a frequency response analyzer. In this paper, we present an innovative diagnostic technique based on analysis of free voltage and current signals to give a so called "quasi-electrochemical impedance spectrum" (QEIS) and demonstrate its application on a Li-ion battery during a real EV duty cycle. It is worth noting that in our technique no additional signal is applied to the cell, since the current flowing into cells during use on-board is directly processed in the data treatment step.

Commercial batteries (1.4 Ah cylindrical $LiFePO_4$/graphite cell) were selected in this study to validate the diagnostic method in the framework of an applied case study related to an electric school bus demonstrator. In order to study the capability of QEIS measurements as a diagnostic tool for SoH of Li-ion cells, a test procedure including ageing phases has been defined to characterise Li-ion cells before and during ageing. Voltage and current signals were treated by Fast Fourier Transform (FFT) in order to determine the QEIS spectra of Li-ion cells under study. Then, SoH prediction algorithms have been obtained from a mathematical analysis of the impedance parameters sensitive to SoH.

1. Introduction

The development of improved State-of-Health (SoH) diagnostic methods is a current research topic for battery-powered applications [1–3]. Due to the rapid development and deployment of Electric Vehicles (EV) there is a strong demand for an accurate and reliable technique for monitoring SoH during operation. Such a technique requires a measurable indicator that can be processed in an embedded system to give a quantitative measure of SoH. This is a key parameter required to optimize battery energy management and to track the degradation of the system performance. In this study, we investigate a novel "quasi electrochemical impedance spectroscopy" (QEIS) technique and apply it to determine SoH of a battery aged with a current profile which mimics the electrical needs of an electric school bus.

Electrochemical impedance spectroscopy (EIS) is a well-known and powerful tool used to analyze [4–6] and model [7–9] electrochemical systems such as batteries. It is a non-invasive technique relying on a small perturbation signal being applied over a wide frequency range, and allows the investigation of internal phenomena with different time constants in a single measurement.

The general principle of the EIS method is to apply to a cell a sinusoidal signal and measure the characteristic response from

* Corresponding author.
E-mail address: Remy.Mingant@ifpen.fr (R. Mingant).

http://dx.doi.org/10.1016/j.apenergy.2016.08.118
0306-2619/

the cell [6]. The applied signal can either be current or voltage. The response $\bar{u}(f)$ (or $\bar{i}(f)$) (complex numbers) are recorded. The impedance $\bar{u}(f)$ is then calculated by using the following equation:

$$\overline{Z}(f) = \frac{\bar{u}(f)}{\bar{i}(f)} \quad (1)$$

Finally, $\overline{Z}$ is a complex vector which can be displayed in a Nyquist plot in order to visualize the influence of the parameters. This frequency-domain analysis requires that the system under investigation is linear or at least can be linearized with respect to signal amplitudes in its working point and is stationary or at least quasi-stationary for the time of measurement. Fitting experimental EIS with an electrical equivalent circuit is a well-known analysis method [10–17]. This fit is generally done with a Levenberg-Marquardt or a simplex method minimizing least-squares between the model and experimental data. The best-fit parameters obtained by this method can then be used to determine an appropriate SoH indicator by mathematical combination to obtain a linear correlation with SoH.

Another method [13] directly uses an electrical equivalent circuit model that depends only on State-of-Charge (SoC) and SoH. Using this method, SoC and SoH can be directly determined by fitting the measured electrochemical impedance spectrum. Several unconventional methods have been developed to measure an EIS spectrum without requiring the often time-consuming application of a single sinusoidal signal at successive frequencies. For example, a so-called "multisine" method comprising several frequencies superposed on a single composite signal can be used to determine an entire spectrum in the time required for the lowest frequency point, giving an almost instantaneous EIS response [18]. This technique requires mathematical tools such as Fourier transform and a sophisticated signal generator for the input signal. A faster technique called dynamic EIS (DEIS) measures the impedance response of lithium-ion batteries during charge/discharge at finite DC currents [19–22]. In this technique, the impedance measurement during charge/discharge, the lithium-ion batteries are subjected to a current consisting of a constant direct current and a small alternating current (AC) perturbation. Furthermore, methods employing a single current step have been studied [23], and another technique using white noise has been tested by Gabrielli et al. [24]. These methods require an input signal which need a battery to be in a rest period, and apply a perturbation on laboratory conditions. Another method, developed by Alavi et al. [25] consisted of estimating simple equivalent circuit model parameters directly from time-domain data. However, application of the method to estimate the EIS model parameters using more complex models is challenging.

In order to avoid the additional burden of an input signal, we have proposed to make use of the free signals of current and voltage from acceleration and regenerative braking that occur during a vehicle road trip [26]. These solicitations of the battery can be very complex and indeed can be considered as an almost random profile. Hence, the current and voltage battery signals could be used to determine a "quasi-EIS" (QEIS) battery spectrum using the method described in previous work [26]. It is worth noting that batteries are usually operated at currents so large that the nonlinearity of transport and reaction processes cannot be neglected. Secondly, batteries change their structure while being discharged or charged, and they are typically operated until at least one species of reactants depletes non-stationarity. For this reason this technique is not considered like EIS. It is expected that this method could be used as an onboard diagnostic tool.

This paper first introduces the vehicle application considered in this work, followed by a specific battery ageing protocol that has been developed to simulate ageing for two vehicle architectures. The QEIS data processing including the electrical modelling with an equivalent circuit is described afterwards and applied to the ageing data generated in our laboratories. Finally a correlation between the capacity losses and QEIS model parameters is established to discuss the practical performance of this novel method as an in-service SoH indicator.

2. Experimental

2.1. Case study

The target application is an electric school bus whose mission is to pick up children in the morning on the way to school, return to the bus station in order to charge the traction battery, and then repeat its mission in the opposite direction in the afternoon. Hence the battery charges and discharges twice a day. The first task in defining the bus demonstrator architecture was to size the Li-ion battery, considering two different cases:

- An 85 kW h battery (so called "one pack") which is sized to discharge until a state of charge of 14% is reached;
- A 170 kW h battery (so called "two packs") which is oversized for the application in order to compensate the capacity loss during ageing.

For these two cases, in-service current profiles were created using an electric vehicle simulator [27] in order to simulate the morning and afternoon school bus tours. These current profiles were then used to define the ageing protocol.

2.2. Materials

Commercial Li-ion batteries (1.4 Ah cylindrical $LiFePO_4$/-graphite Valence Technology cells) were selected at the beginning of the project to reversibly store electrical energy in the electric school bus. The nominal cell voltage is 3.3 V and voltage limits are 2.5 V and 3.6 V. Two modules of 66 cells in parallel were available for the study.

2.3. Ageing method

Ageing campaigns were launched at module level to collect battery voltage and current data with time, at various SoH. The ageing protocol is intended to provoke both capacity fading and an increase in internal resistance in the batteries. Thus, regular measurements of battery capacity and internal resistance, so called check-up, are mandatory alongside ageing campaigns. The check-up procedure involves significant perturbations on the battery, so in order to limit the impact of the check-up phases on the battery ageing, 3 cells were removed from each module to perform a full check-up at cell level and get a statistical determination of SoH from three samples. Then, the ageing protocol continued on the remaining cells of the battery pack with the current profile adapted for the remaining number of cells.

Two electrical test benches were used at IFPEN facilities: a Digatron power test bench 200 A/50 V (±10 kW) associated with a large climatic chamber was used to age battery modules submitted to dynamic current cycles under controlled ambient temperature. Module voltage and temperature were measured by the test bench and recorded on a computer. The periodic check-up experiments were carried out on individual cells using a Bio-logic VMP3 multi-channel potentiostatic-galvanostatic system equipped with an impedance module (BioLogic Science Instruments, France).

Fig. 1 presents the current profiles simulating the morning tour for the "one pack" and "two packs" cases. Each module under test

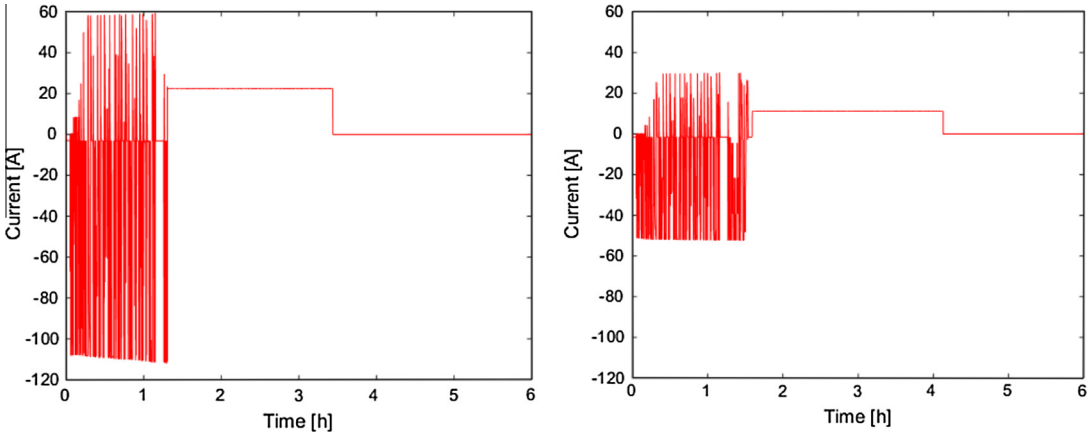

Fig. 1. Ageing current profiles for 1 pack (a), 2 packs case study (b) (generated by IFPEN simulation platform [27]).

was placed into the climatic chamber set to 45 °C and connected to the battery test bench system. Fig. 2 represents the cycling procedure of the two modules. On this figure, the full charge is done at C/3 and C/6 current rate for respectively the "one pack" and "two packs" cases until the voltage reaches 3.6 V. Then, the battery is charged at current voltage until the complete time of charging of 2 h 35 min. In this figure, the cycle profile 1 is the morning cycle, and the cycle profile 2 the afternoon profile the cycling procedure was looped for a total of 7 months for each module. Every month, both modules were submitted to a check-up, and 3 cells were removed from both modules and individually submitted to a check-up.

The module check-up procedure consisted of full charge/discharge cycling at C/3 rate and 25 °C in order to determine the residual module capacity. The modules were then totally discharged to allow the safe removal of 3 cells. Once the 3 cells were removed, the module was heated back to 45 °C and submitted to ageing cycling again but with an adapted current.

The full check-up performed on the removed cells consisted of four charge/discharge cycles at C rate to determine the capacity of each cell, followed by HPPC(Hybrid Pulse Power Characterization) profiles in 15 points: from SoC = 100% with a long rest period, cell undergoes a first EIS measurement following the procedure detailed in Fig. 3. This procedure was looped for 15 times. All capacity and resistance measurements were performed at 25 °C.

2.4. QEIS determination

The principle of EIS is to measure the complex electrochemical impedance of a cell as a function of frequency. The conventional method consists of the excitation of the electrochemical cell with a sinusoidal current (or voltage) and the measurement of the voltage (or current) response. By applying a small amplitude input signal a linear relationship can be assumed for the response. This procedure is repeated for each frequency studied. Thus, the complex impedance Z is calculated with the formula (1):

$$Z(f) = |Z| \cdot e^{i\varphi_z} = \left|\frac{U(f)}{I(f)}\right| e^{i\varphi_z} \tag{2}$$

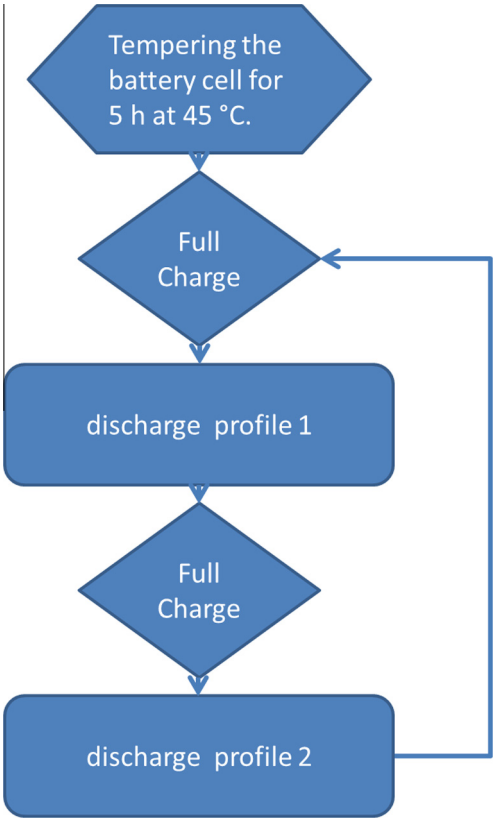

Fig. 2. Ageing procedure of modules.

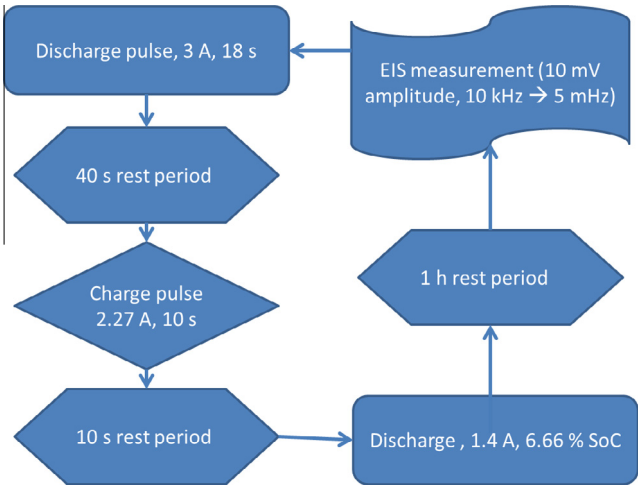

Fig. 3. Check-up procedures of individual cells.

where f is the frequency, U is the voltage amplitude, I, the current amplitude, and φ_z the phase shift between both U and I.

The power spectral density (PSD) is a mathematical function generally used to represent the different spectral components of a signal. It is equal to the square of the modulus of the Fourier transform of X(t), denoted X(f) reported in half the acquisition time (2):

$$\Psi_x(f) = \frac{2}{T}|X(f)|^2 \tag{3}$$

where T is the integration time.

The PSD represents the distribution of frequencies present in the signal, hence a perfect white noise signal would constitute a constant PSD at all frequencies. There are also cross-power spectral densities which are composed of a combination of two Fourier transforms X(f) and Y(f) (3):

$$\Psi_{xy}(f) = \frac{2}{T}X(f)Y^*(f) \tag{4}$$

An example of PSD curves measured during road cycling of a battery is presented in Fig. 4. As shown in this figure, the PSD of this road-cycling protocol consists of two parts: a low-frequency plateau ($f < 0.01$ Hz), followed by a decrease at increasing frequencies.

The impedance Z is classically calculated using the formula (4), rearranged for its calculation from PSD (?):

$$Z(f) = \frac{V(f)}{I(f)} = \frac{\frac{2}{T}V(f)I^*(f)}{\frac{2}{T}I(f)I^*(f)} = \frac{\Psi_{IV}(f)}{\Psi_I(f)} \tag{5}$$

However, this formula does not practically provide a good accuracy of the impedance, because of the noise of the measurement. It is therefore necessary to divide the signal into N blocks, then to take the average before calculating the impedance (5).

$$\mathrm{Z(f)} = \frac{\frac{1}{N}\sum_{j=1}^{N}\frac{2}{T}\mathrm{V_j}(f)\mathrm{I_j^*}(f)}{\frac{1}{N}\sum_{j=1}^{N}\frac{2}{T}\mathrm{I_j}(f)\mathrm{I_j^*}(f)} = \frac{\frac{1}{N}\sum_{j=1}^{N}\Psi_{UI}(f)}{\frac{1}{N}\sum_{j=1}^{N}\Psi_I(f)} \tag{6}$$

This division of blocks causes a reduction of the number of studied frequencies, because of the decrease in the amount of information processed at any time. Thus, for a sample of n values, measured at constant time step, Δt, the frequency f is a vector comprising the numbers from 1 to n, divided by the duration of the test. Thus, a reduction in sample size also results in a reduction of the number of frequencies by decreasing the number of low frequencies.

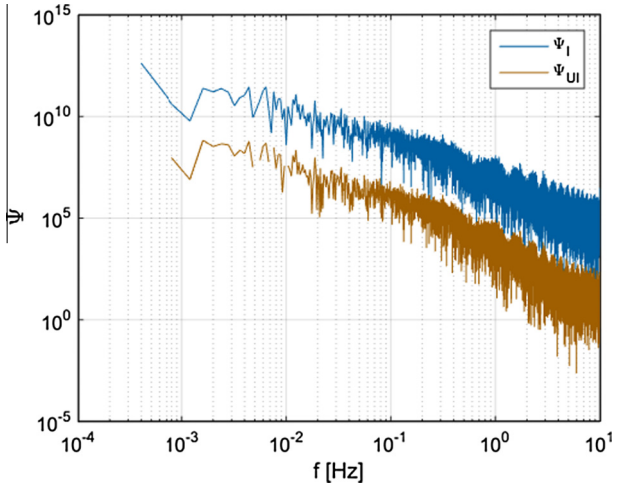

Fig. 4. PSD of during road cycling phase of the one pack ageing.

In addition, according to the Nyquist-Shannon theorem, higher frequencies must be removed to ensure accurate rendering of the signal by limiting aliasing effects (which reduces even more the number of frequencies of study). Then, the number of studied frequencies is reduced by at least a factor of 2.

There is an important source of uncertainty to consider arising from the signal. This analysis method ideally requires a white noise input signal, but the real-world power cycle in this application is clearly not an ideal white noise, and thus the power spectral density is not constant with frequency (as can be seen in Fig. 4). The implication of this is that the impedance spectrum calculated from the ratio U(f)/I(f) contains a significant random uncertainty. This can be seen in Fig. 5a which shows the result of a direct calculation of Z from the 80,000 values of Ψ(U)/Ψ(I) in Fig. 4. The basic shape of a semicircular EIS spectrum can be imagined in this figure but there is an unacceptable level of noise in the pattern. Thus, to improve the correlation with a conventional EIS result, a filter system of the power spectral density has been developed. This filter consists to select frequencies of which the current is higher, so dissociated from the noise (Fig. 5b). Hence, the filter selects the impedance of which the index correspond to a PSD current (PSDI) greater than (PSDI max)/10.

In order to increase even more the relative accuracy of the electrochemical impedance, it was then proposed to cut the signal to reduce the number of points and the electrochemical noise. One solution is to treat the same signal several times, but with a "cutting" becoming smaller. As an example for the voltage signal (x values) on Fig. 6: the first cutting presents 2 sections of x/2 values each (and then processing with the previous algorithm), the second cutting presents 4 sections of x/4, the third one, 8 sections of x/8, etc, the end of the cutting represent the one in which the size of the section is under 32 values.

It is worth noting that this type of treatment does not allow obtaining impedance spectra on the same frequency range as a standard measurement made from sinusoids (Fig. 7).

2.5. Accuracy study

In order to develop a diagnosis tool, it is necessary to quantify the measurement accuracy to assess the performance of the method. In our study, given the measurement accuracy of both the input current and the output voltage, the measurement error can be considered as a parasitic noise. Thus, according to Gabrielli et al. [24], "the presence of parasitic noise for a low-amplitude signal either increase the measurement time or reduce the measurement accuracy". In this paper, the relative estimation errors $\in(|\widehat{Z}|)$, which will simply be called errors, are defined by:

$$\in^2\left(|\widehat{Z}|\right) \leqslant \frac{1}{2N}\left(\frac{1}{\eta_i} + \frac{1}{\eta_v}\right) \tag{7}$$

where η_i and η_v are respectively the signal-to-noise ratios (current) at the input and at the output, N is the number of blocks. The accuracy measurement is $\in_v = 10$ mV for the voltage and $\in_i = 0.5$ A for the current. The signal-to-noise ratios can be defined by:

$$\eta_i(f) = \frac{|I(f)|}{\in_i} \text{ and } \eta_v(f) = \frac{|U(f)|}{\in_v} \tag{8}$$

where U(f) is the voltage amplitude and I(f), the current amplitude.

Fig. 8 shows an impedance spectrum of an LFP/C 1.4 Ah cell obtained from the QEIS. The calculated error bars according to Eq. (1) are depicted in red. On this plot, one can observe that the error on impedance measurement is larger at high frequency than at lower frequency, ranging respectively from ±4 mΩ to 2 mΩ. Indeed, according to the PSD plot on Fig. 4, the PSD is higher at low frequency leading to a higher signal-to-noise ratio.

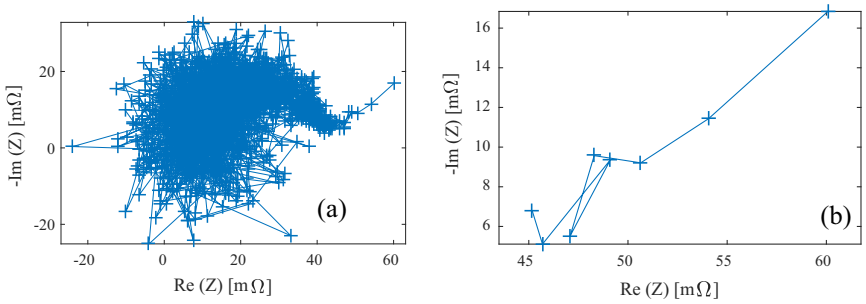

Fig. 5. Electrical Impedance spectrum of the LFP/C 1.4 Ah cell from an EV profile without DSP filter (a), and with DSP filter (b).

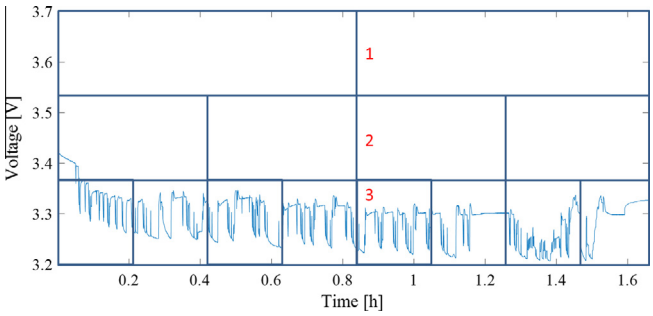

Fig. 6. Representation of the cutting phases of a signal.

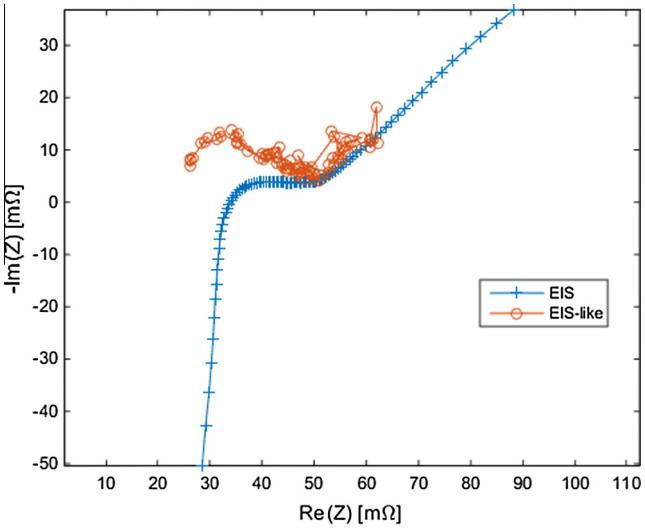

Fig. 7. Impedance spectra of an LFP/C 1.4 Ah cell obtained from the QEIS method with "successive cutting" from a signal [U, I] = f (t) road (frequencies of 0.78 to 0.015 Hz), compared with Nyquist spectrum measured on a similar cell at the same temperature (frequencies from 10 000 to 0.005 Hz).

In conclusion of this part, on the whole range of QEIS measurement, a maximal error of 4 mΩ represents a maximal relative error of 10%. It permits us however to fit correctly the shape of the impedance with an equivalent circuit based model.

2.6. QEIS data processing (equivalent circuit based model)

A generic electrical equivalent circuit was used to model Li-ion battery EIS spectra and is shown in Fig. 9. This circuit includes one ohmic series resistance R0 which represents electrolyte resistance. The charge transfer resistance is represented by a parallel branch consisting of a capacitance C1 and a resistance R1. Finally, diffusion

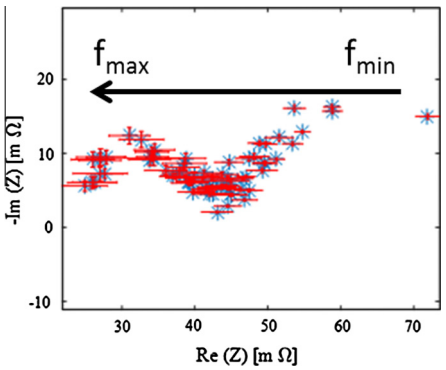

Fig. 8. Electrical Impedance spectrum of the LFP/C 1.4 Ah cell from an EV profile, blue (∗), QEIS, red (−), error bars calculated with Eq. (7). (For interpretation of the references to colour in this figure legend, the reader is referred to the web version of this article.)

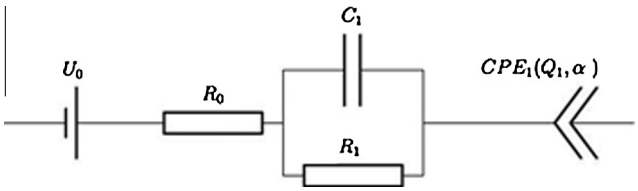

Fig. 9. Electrical equivalent circuit for QEIS spectra fitting.

is represented by a constant phase element (CPE) in which α and Q1 are additional fit parameters. In this way the dynamic electrical characteristics of the battery can be modelled using basic electrical components, like resistors and capacitors, and the fitting parameters can be empirically correlated to the battery SoH.

3. Results

3.1. Ageing campaign

Fig. 10 shows the voltage values of modules measured during the ageing cycle in both pack cases under study. In these plots, lines can be observed every 30 days which correspond to full discharge and charge between check-ups. The first plot relates to the "two packs" case study, and exhibits almost no voltage evolution between the first and the last cycling, implying that there is no significant ageing. By contrast, the second plot obtained for the "one pack" case study shows that the minimum discharged voltage of the module decreases to reach the minimal rated voltage of the cell, namely 2.5 V, after only 55 ageing days. At this point, the full battery would not be able to fulfil the theoretical bus mission, but for the sake of this study the ageing test was continued. For this

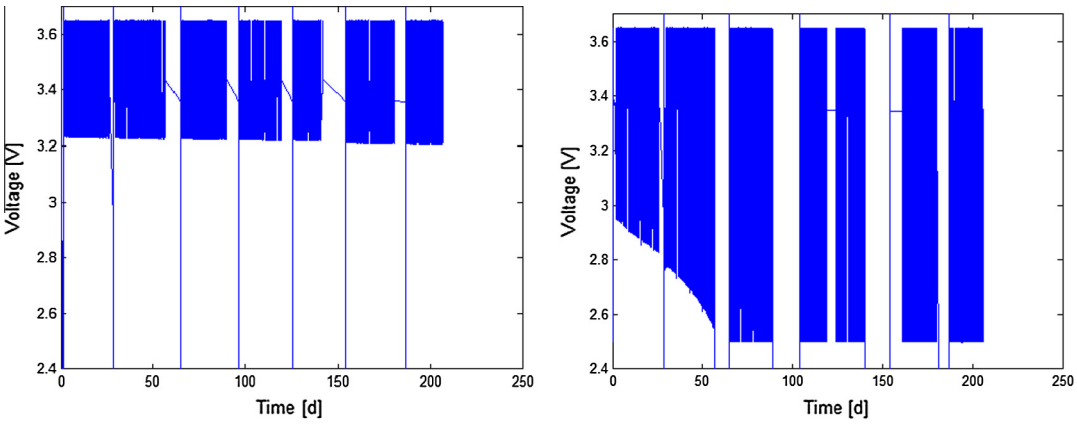

Fig. 10. Module voltage evolution with time during ageing tests for different current profiles corresponding to both case studies under consideration (left, 2 packs case, right 1 pack case).

test the cycling procedure was the same, but the battery discharge stopped at a battery voltage of 2.5 V.

Fig. 11 shows the capacity fade for the modules in the two different sizing scenarios. After an initial increase in capacity, both modules follow an approximately linear capacity fade with time. Consistent with the previous figure, the module representing the "one pack" case exhibits the fastest degradation, with 20% of capacity fade after 210 ageing days, while the "two packs" module undergoes a less severe degradation with 10% of capacity fade after 210 ageing days.

3.2. QEIS compared to EIS during ageing

In order to discuss the impact of SoH on electrochemical impedance spectra, EIS and QEIS spectra have been graphically compared in Figs. 12 and 13 using the Nyquist representation on the same frequency range. The EIS measurements were taken from the individual cells removed for full check-up every 30 days in Fig. 12, while the QEIS spectra of the modules from three stages of the ageing test are shown in Fig. 13. One can observe that the spectrum moves to the right side as the battery ages, which is indicative of an increase in the ohmic resistance R0 as reported in the literature for classical Li-ion ageing characteristics [28]. According to this previous work, during ageing a surface film irreversibly grows on the graphite electrode (known as the Solid Electrolyte Interphase). This film is electrically insulating, which accounts for the increase in ohmic resistance. A comparison between two study cases shows a faster increase of the ohmic resistance with the first configuration than for the two pack case. This reflects a more severe ageing for the one pack case.

Similarly, the QEIS measurements given in Fig. 13 show that the spectrum moves to the right side as the battery ages, which indicates that a qualitative correlation can be directly observed between the two techniques.

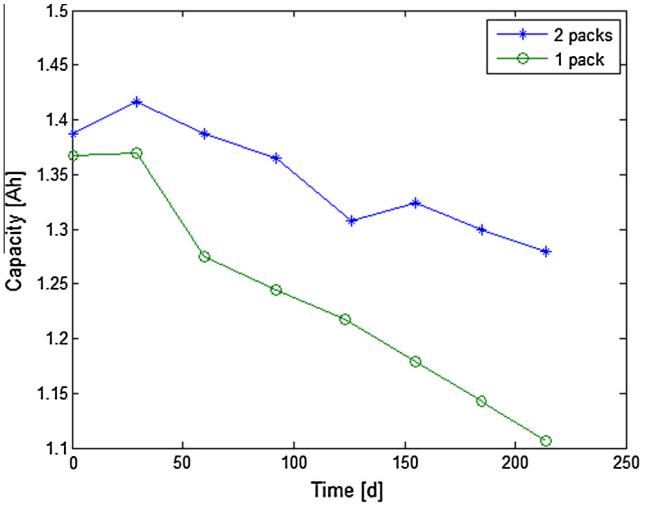

Fig. 11. Comparison of the measured module capacity (in Ah/cell) during cycling for 2 packs and 1 pack cases.

3.3. QEIS spectrum modelling

Since there is clearly some inherent uncertainty remaining in the QEIS results, fitting the electrical equivalent circuit model could lead to erroneous results if all the parameters were left free to vary in the fitting algorithm. For this reason, some parameters were set constant as a function of SoH (Table 1), based on the fitting results obtained from all the QEIS measurements. R1 and Q1 parameters have been allowed to vary with SoH, this low frequency impedance is related to a combined effect of the diffusion of lithium ions on the electrode–electrolyte interfaces, which corresponds to the straight sloping line observed in the Nyquist plot towards low frequencies [29].

Fig. 14 illustrates an example of a QEIS spectrum fitted with the equivalent circuit model. One can observe a qualitative satisfying adjustment of the QEIS spectrum with the electrical equivalent circuit as previously defined. Fitted parameters obtained on the module at 25 °C before ageing have been gathered in Table 2. Later in this paper we will use these fitted parameters in order to determine the module's SoH.

3.4. SoH diagnostic

SoH is considered as the ratio between the real capacity and the initial capacity. The next step of this study is to compare fitted parameters for both ageing campaigns as a function of capacity fade.

The "one pack" case has obviously induced a more severe ageing effect on the module than the "two packs" case, which is expected due to the substantially higher mean current and larger SoC range encountered in the "one pack" case study, and as already noted in Fig. 11. Fig. 15 shows the increase of the ohmic resistance R0 for the two aged modules as a function of capacity fade, which is thought to be related to SEI growth as already discussed. Fig. 16

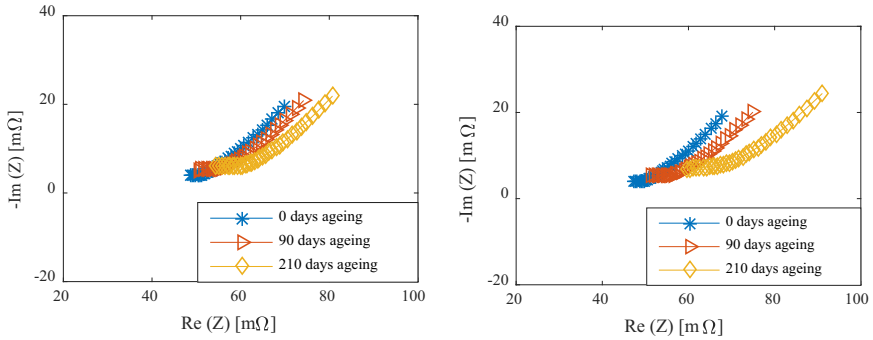

Fig. 12. Conventional EIS spectra of the LFP/C 1.4 Ah cell obtained during check-up at 25 °C with 2 packs and 1 pack cases.

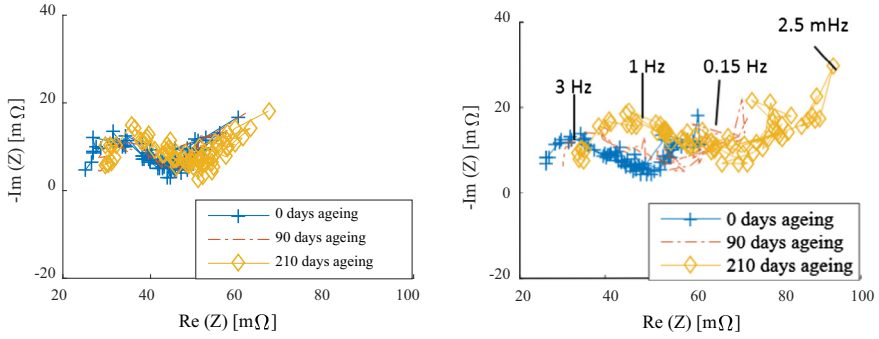

Fig. 13. QEIS spectra of the LFP/C 1.4 Ah cell obtained during cycling at 45 °C with 2 packs and 1 pack cases.

Table 1
Constant values used on the model to fit interest parameters.

Parameter	R_0 [mΩ]	C1 [F]	α
Value	22.2	11.4	0.5

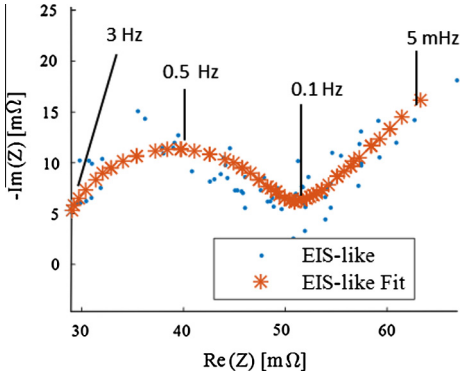

Fig. 14. Example of Nyquist curve fitted with equivalent circuit model.

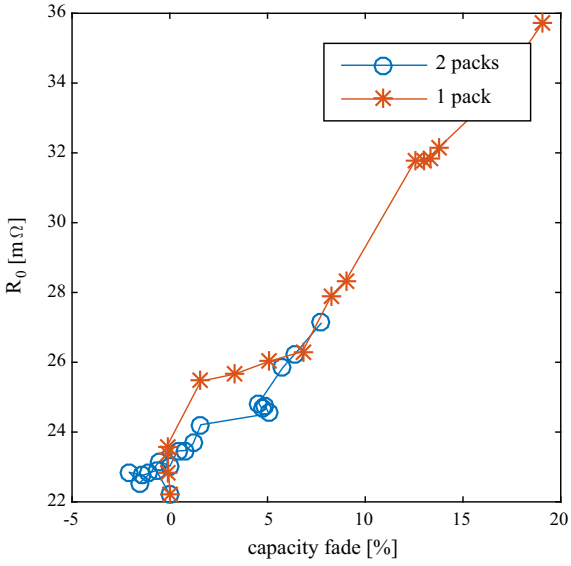

Fig. 15. R0 vs. capacity fade (modules).

Table 2
QEIS results obtained on the module @25 °C before ageing.

	R_0 [mΩ]	R_1 [mΩ]	Q1 [$F^{0.5}$]
1 pack	22.2	17.8	297
2 packs	22.2	21.8	336

shows the decrease in the Q1 coefficient of the CPE element as a function of capacity fade.

Fitted parameters R0 and Q1 both show a monotonic evolution with capacity fade but opposite trends. However, these fitted parameters cannot satisfactorily be directly used to predict capacity fade: for R0, the two curves diverge between 0% and 5% of capacity fade; and for Q1, the curves are parallel, but not superposed. In order to have an indicator, the combination, $\frac{R_0}{Q_1}$, was considered as a function of capacity fade as illustrated in Fig. 17. According to this figure, the superposition is reasonably effective for both current profiles, revealing that a unique mechanism governs the ageing features under consideration, such as capacity fade, in "one pack" and "two packs" cases. When the "one pack and two packs" $\frac{R_0}{Q_1}$ curves are superposed, the proposed indicator could

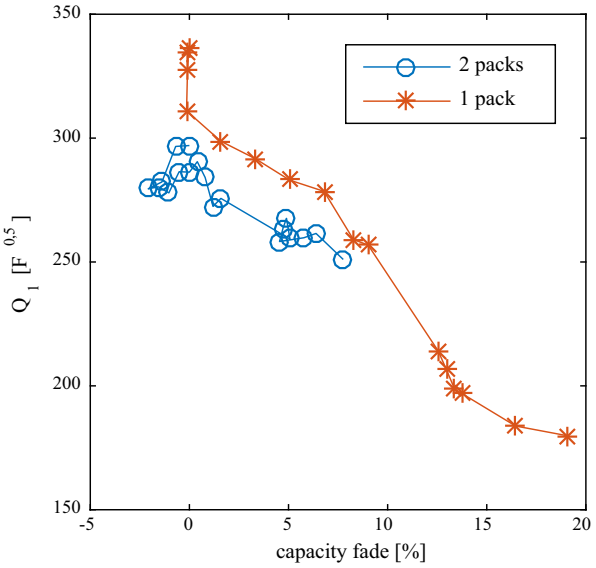

Fig. 16. Q1 vs. capacity fade (modules).

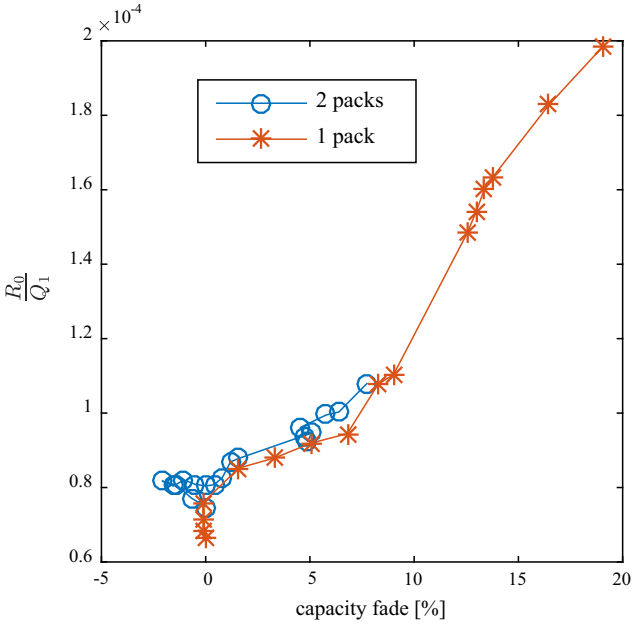

Fig. 17. R0/Q1 vs. SoH.

predict module capacity fade with a 2% uncertainty (calculated as the largest gap between the two curves). It is worth noting that the effect of temperature has not yet been taken into account in this study, but this could be considered using an Arrhenius law to extend the predictability of the R0/Q1 correlation with capacity fade as SoH indicator.

4. Conclusions

In this study, a new *in operando* method for estimating the SoH of a Li-ion battery was assessed on a commercial module. The method uses the real current and voltage values of the module during an in-use load cycling scenario as input data to calculate an impedance spectrum, so-called QEIS, which could be fitted to an electrical equivalent circuit model. SoH prediction algorithms have been obtained from a mathematical analysis of the model parameters.

This method has been applied to ageing data collected from two modules undergoing different ageing protocols over 7 months. QEIS spectra calculated using our method were fitted to an electrical equivalent circuit model. It was found that the ohmic resistance (R0) and capacitance (C1) parameters of the model evolved monotonically with capacity fade of the battery, for the two different ageing protocols under consideration. By combining the two parameters an indicator of battery SoH was obtained, measurable using only the free output signals of the battery (current and voltage). This correlation could further be applied to other Li-ion battery systems, provided there is a similar ageing mechanism triggered. This method is a promising solution for an embedded system to monitor battery SoH and also for lifetime prediction. To be used for another Li-ion technology it is however necessary to process to a measurement campaign in order to evaluate adapted fitted parameters of other battery chemistries.

Acknowledgments

Authors wish to gratefully acknowledge the French FUI for supporting the SCOLELEC project.

References

[1] Ozkurt C, Camci F, Atamuradov V, Odorry C. Integration of sampling based battery state of health estimation method in electric vehicles. Appl Energy 2016;175:356–67.
[2] Omar N, Monem MA, Firouz Y, Salminen J, Smekens J, Hegazy O, et al. Lithium iron phosphate based battery–assessment of the aging parameters and development of cycle life model. Appl Energy 2014;113:1575–85.
[3] Hu C, Jain G, Tamirisa P, Gorka T. Method for estimating capacity and predicting remaining useful life of lithium-ion battery. Appl Energy 2014;126:182–9.
[4] Dolle M, Orsini F, Gozdz AS, Tarascon JM. Development of reliable three-electrode impedance measurements in plastic Li-ion batteries. J Electrochem Soc 2001;148(8):A851–7.
[5] Zhai NS, Li MW, Wang WL, Zhang DL, Xu DG. The application of the EIS in Li-ion batteries measurement. J Phys: Conf Ser 2006;48:1157–61.
[6] Andre D, Meiler M, Steiner K, Wimmer C, Soczka-Guth T, Sauer DU. Characterization of high-power lithium-ion batteries by electrochemical impedance spectroscopy. I. Experimental investigation. J Power Sources 2011;196(12):5334–41.
[7] Buller S, Karden E, Kok D, De Doncker RW. Modeling the dynamic behavior of supercapacitors using impedance spectroscopy. IEEE Trans Ind Appl 2002;38 (6):1622–6.
[8] Buller S, Thele M, Karden E, De Doncker RW. Impedance-based non-linear dynamic battery modeling for automotive applications. J Power Sources 2003;113(2):422–30.
[9] Montaru M, Pélissier S. Frequency and temporal identification of a Li-ion polymer battery model using fractional impedance. Oil Gas Sci Technol J 2010;65(1):67–78.
[10] Troltzsch U, Kanoun O, Trankler HR. Characterizing aging effects of lithium ion batteries by impedance spectroscopy. Electrochim Acta 2006;51(8):1664–72. http://dx.doi.org/10.1016/j.electacta.2005.02.148.
[11] Andre D, Meiler M, Steiner K, Walz H, Soczka-Guth T, Sauer DU. Characterization of high-power lithium-ion batteries by electrochemical impedance spectroscopy. II: Modelling. Selected papers presented at the 12th Ulm ElectroChemical Talks (UECT):2015 technologies on batteries and fuel cells 2011;196(12):5349–56.
[12] Kim J, Cho BH. An innovative approach for characteristic analysis and state-of-health diagnosis for a Li-ion cell based on the discrete wavelet transform. J Power Sources 2014;260:115–30.
[13] Mingant R, Bernard J, Sauvant-Moynot V. In-situ battery giagnosis method using electrochemical impedance spectroscopy; FR20100003820; 2012.
[14] Bernard J, Delaille A, Huet F, klein JM, Mingant R, Sauvant-Moynot V. Methode de diagnostic in-situ de batteries par spectroscopie d'impedance electrochimique(FR2956486 A1); 2011.
[15] Galeotti M, Giammanco C, Cinà L, Cordiner S, Di Carlo A. Synthetic methods for the evaluation of the State of Health (SOH) of nickel-metal hydride (NiMH) batteries. Energy Convers Manage 2015;92:1–9.
[16] Abdel Monem M, Trad K, Omar N, Hegazy O, Mantels B, Mulder G, et al. Lithium-ion batteries: evaluation study of different charging methodologies based on aging process. Appl Energy 2015;152:143–55.
[17] Waag W, Käbitz S, Sauer DU. Experimental investigation of the lithium-ion battery impedance characteristic at various conditions and aging states and its influence on the application. In: Special issue on advances in sustainable

biofuel production and use – XIX International Symposium on Alcohol Fuels – ISAF, vol. 102; 2013. p. 885–97.
[18] Breugelmans T, Lataire J, Muselle T, Tourwé E, Pintelon R, Hubin A. Odd random phase multisine electrochemical impedance spectroscopy to quantify a non-stationary behaviour: theory and validation by calculating an instantaneous impedance value. Electrochim Acta 2012;76:375–82.
[19] Diard J-P, Le Gorrec B, Montella C. EIS study of electrochemical battery discharge on constant load. J Power Sources 1998;70(1):78–84.
[20] Huang J, Ge H, Li Z, Zhang J. Dynamic electrochemical impedance spectroscopy of a three-electrode lithium-ion battery during pulse charge and discharge. Electrochim Acta 2015;176:311–20.
[21] Karden E, Buller S, De Doncker RW. A method for measurement and interpretation of impedance spectra for industrial batteries. J Power Sources 2000;85(1):72–8.
[22] Itagaki M, Kobari N, Yotsuda S, Watanabe K, Kinoshita S, Ue M. In situ electrochemical impedance spectroscopy to investigate negative electrode of lithium-ion rechargeable batteries. J Power Sources 2004;135(1–2):255–61.
[23] Gabrielli C, Huet F, Keddam M, Lizee JF. Measurement time versus accuracy trade-off analyzed for electrochemical impedance measurements by means of sine, white noise and step signals. J Electroanal Chem 1982;138(1):201–8.
[24] Gabrielli C, Huet F, Keddam M. Comparison of sine wave and white noise analysis for electrochemical impedance measurements. J Electroanal Chem 1992;335(1–2):33–53.
[25] Alavi SMM, Birkl CR, Howey DA. Time-domain fitting of battery electrochemical impedance models. J Power Sources 2015;288:345–52.
[26] Mingant R, Bernard J, Sauvant-Moynot V, IFP Energies nouvelles. Procédé non intrusif de determination de l'impedance électrique d'une batterie; FR20100000778(FR2956743 A1); 2011.
[27] Badin F, Le Berr F, Briki H, Dabadie J, Petit M, Magand S, et al. Evaluation of EVs energy consumption influencing factors, driving conditions, auxiliaries use, driver's aggressiveness. In: World electric vehicle symposium and exposition (EVS 27), 2013, Barcelona, Spain, 17–20 November 2013. Piscataway, NJ: IEEE; 2013. p. 1–12.
[28] Gyan P, Aubret P, Hafsaoui J, Sellier F, Bourlot S, Zinola S, et al. Experimental assessment of battery cycle life with in the SIMSTOCK research program. Oil Gas Sci Technol-Rev IFP Energies Nouv 2013;68(1):137–47.
[29] Zhang SS, Xu K, Jow TR. Electrochemical impedance study on the low temperature of Li-ion batteries. Electrochim Acta 2004;49(7):1057–61.